Journal of Rock Mechanics and Geotechnical Engineering 16 (2024) 990–999

Contents lists available at ScienceDirect

Journal of Rock Mechanics and Geotechnical Engineering

journal homepage: www.jrmge.cn

Full Length Article

Soil disturbance evaluation of soft clay based on stress-normalized small-strain stiffness

Yanguo Zhou [a,*], Yu Tian [a], Junneng Ye [b], Xuecheng Bian [a], Yunmin Chen [a]

[a] MOE Key Laboratory of Soft Soils and Geoenvironmental Engineering, Institute of Geotechnical Engineering, Center for Hypergravity Experiment and Interdisciplinary Research, Zhejiang University, Hangzhou, 310058, China
[b] Ningbo Rail Transit Group Co., Ltd., Ningbo, 315010, China

ARTICLE INFO

Article history:
Received 30 January 2023
Received in revised form
27 June 2023
Accepted 14 August 2023
Available online 3 December 2023

Keywords:
Natural clay
Soil sample disturbance
Shear wave velocity
Small-strain shear modulus
Hardin equation

ABSTRACT

Soil disturbance includes the change of stress state and the damage of soil structure. The field testing indices reflect the combined effect of both changes and it is difficult to identify the soil structure disturbance directly from these indices. In the present study, the small-strain shear modulus is used to characterize soil structure disturbance by normalizing the effective stress and void ratio based on Hardin equation. The procedure for evaluating soil sampling disturbance in the field and the further disturbance during the subsequent consolidation process in laboratory test is proposed, and then validated by a case study of soft clay ground. Downhole seismic testing in the field, portable piezoelectric bender elements for the drilled sample and bender elements in triaxial apparatus for the consolidated sample were used to monitor the shear wave velocity of the soil from intact to disturbed and even remolded states. It is found that soil sampling disturbance degree by conventional thin-wall sampler is about 30% according to the proposed procedure, which is slightly higher than that from the modified volume compression method proposed by Hong and Onitsuka (1998). And the additional soil disturbance induced by consolidation in laboratory could reach about 50% when the consolidation pressure is far beyond the structural yield stress, and it follows the plastic volumetric strain quite well.

1. Introduction

Soil structure refers to the shape and arrangement of soil particles and voids, as well as the interaction of forces between soil particles. It is produced by various physical and chemical processes of natural soils during and after deposition (Mitchell, 1970). Most natural sedimentary soils, especially soft clays, have different degrees of structure, which makes the compression and consolidation characteristics, stress-strain relationships, the cyclic behavior, stiffness and strength parameters and other engineering properties significantly different from reconstituted soils (Rampello and Callisto, 1998; Hight and Leroueil, 2002; Nagaraj et al., 2003; Low and Phoon, 2008; Hong et al., 2012; Zeng and Hong, 2015; Xiong et al., 2018; Jana and Stuedlein, 2020; Khalid et al., 2021; Tanoli and Ye, 2021; Dadashiserej et al., 2022). Soil structure disturbance refers to plastic deformation, sliding of soil particles, destruction of metastable structure, and chemical cementation after being disturbed. The commonly observed soil disturbance problems include sampling disturbance and construction disturbance, which may cause additional settlement and various engineering hazards. Therefore, quantitative evaluation of soil disturbance is of great importance. Soil disturbance within soil element includes the elastic strain induced by stress change and the plastic strain corresponding to structure damage. As the elastic strain could be restored by subsequent stress change processes either in laboratory or at construction site, the main challenge becomes the evaluation of soil structure disturbance due to plastic strain.

For soil sampling disturbance evaluation in the laboratory, Hong and Onitsuka (1998) proposed a method to calculate sampling disturbance degree based on the inherent compression line of remolded soil proposed by Burland (1990), and took the compression characteristics of remolded soils as the reference. Similarly, Lunne et al. (2006) and Dejong et al. (2018) evaluated soil sampling quality according to the change of void ratio (i.e. $\Delta e/e_0$). These methods based on laboratory consolidation tests directly

* Corresponding author.
E-mail address: qzking@zju.edu.cn (Y. Zhou).
Peer review under responsibility of Institute of Rock and Soil Mechanics, Chinese Academy of Sciences.

https://doi.org/10.1016/j.jrmge.2023.08.019

correspond to the plastic strain of soil sample and therefore are physically appropriate for soil disturbance evaluation.

On the other hand, there are several other soil disturbance evaluation methods by using engineering parameters from field testing indices, such as the field vane shear strength, which is a mixed reflection of the initial structural state at small strain and the subsequent failure state at large strain, and its capability to characterize the initial structural state is not so good as that of the small-strain shear modulus (G_{max}) at level of $\gamma \leq 10^{-5}$ (as shown in Fig. 1). However, as G_{max} is affected by soil structure, stress state, void ratio and other factors (Hardin and Blandford, 1989; Viggiani and Atkinson, 1995), the direct use of G_{max} to evaluate soil disturbance could not consider the effect of the change of effective stress. For example, Landon et al. (2007) used the ratio between the unconfined shear wave velocity and the in situ shear wave velocity to evaluate soil sampling quality, but such method could not distinguish the proportion of structure damage from stress release in sampling disturbance.

To address this problem, Hardin equation is used to normalize the effective stress and void ratio to obtain the soil structural parameter, and a new method is proposed to evaluate soil structure disturbance based on the concept of disturbance state proposed by Desai and Toth (1996). Then the proposed method is used to calculate the sampling disturbance degree of thin-wall sampled soft soil, and compared with the modified volumetric compression method proposed by Hong and Onitsuka (1998). The subsequent structure disturbance of soil specimen consolidated in triaxial apparatus equipped with bender elements is also evaluated by this method.

2. Soil disturbance evaluation based on small-strain stiffness

2.1. Relationship between soil structure and small-strain shear modulus

The small-strain shear modulus G_{max} is the maximum shear modulus of soil under very small shear strain (e.g. $\gamma \leq 10^{-5}$). Then the small-strain shear modulus is obtained according to elastic theory as follows:

$$G_{max} = \rho V_s^2 \tag{1}$$

where ρ is the bulk density of soil, and V_s is the shear wave velocity.

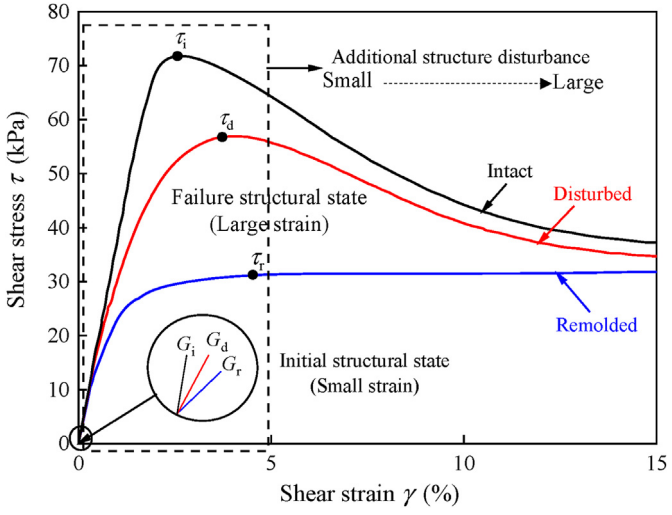

Fig. 1. Schematic diagram of soil disturbance at wide strain range.

Considering that in situ soil is under anisotropic stress states, G_{max} may be expressed as follows (Jamiolkowski et al., 1995):

$$G_{max} = S_{vh} F(e) P_a^{1-n_v-n_h} (\sigma'_v)^{n_v} (\sigma'_h)^{n_h} \tag{2}$$

where S_{vh} is a material parameter reflecting the current soil structure, including soil mineral and particle features; σ'_v is the vertical effective stress; σ'_h is the horizontal effective stress; n_v and n_h are the exponents and could be reasonably assumed $n_v = n_h = n$ (Shibuya et al., 1997); P_a is the atmospheric pressure; and $F(e)$ is the void ratio function and it has the following form according to Lo Presti (1989):

$$F(e) = e^{-x} \tag{3}$$

where x is a fitting parameter.

The small-strain shear modulus is closely related to soil structure (Santamarina et al., 2001; Li et al., 2023). Shibuya et al. (1997) compared the shear modulus of in situ soil, disturbed soil and remolded soil, and found that the change of stress state has basically the same effect on the shear modulus of soil at different disturbance states, while soil structure has an important effect on the shear modulus. Therefore, the small-strain shear stiffness, or shear wave velocity, is a constant-fabric measurement at a given state of stress. If Eq. (2) is further normalized with regard to the effective stress and void ratio, the normalized small-strain shear modulus could solely stand for the structure parameter S_{vh} and then be capable of evaluating soil structure quantitatively.

2.2. Soil structure disturbance evaluation in soft clay

Previous studies have shown that soil structure parameter $S_{vh,r}$ at remolded state, stress exponent n and fitting parameter x of Hardin equation could be determined by laboratory tests of remolded soil (Jamiolkowski et al., 1995). For the same kind of soft clay, n and x are constants independent of soil disturbance state and stress levels. In particular, Shibuya (2000) stated that natural soil structure is reflected by the difference of S_{vh} between the natural and the corresponding remolded soil samples when the (e, p) state is the same.

In order to describe the complete disturbance state based on the disturbance state concept (DSC) proposed by Desai and Toth (1996), the following equations are proposed to evaluate the degree of soil structure disturbance:

$$SDD = \frac{S_{vh,i} - S_{vh,d}}{S_{vh,i} - S_{vh,r}} \times 100\% \tag{4}$$

where SDD is the degree of soil structure disturbance, which ranges from 0 to 100%; $S_{vh,i}$, $S_{vh,d}$ and $S_{vh,r}$ are the structure parameters corresponding to the intact, the disturbed and the remolded soil states, respectively, and they are defined as follows:

$$S_{vh,i} = \frac{G_{max,i}}{F(e_i)\left(\sigma'_{v,i}\sigma'_{h,i}\right)^n P_a^{1-2n}} \tag{5}$$

$$S_{vh,d} = \frac{G_{max,d}}{F(e_d)\left(\sigma'_{v,d}\sigma'_{h,d}\right)^n P_a^{1-2n}} \tag{6}$$

$$S_{vh,r} = \frac{G_{max,r}}{F(e_r)\left(\sigma'_{v,r}\sigma'_{h,r}\right)^{n} P_a^{1-2n}} \tag{7}$$

where $G_{max,i}$, $G_{max,d}$ and $G_{max,r}$ are the small-strain shear moduli of the intact, disturbed and remolded soil, respectively; e_i, e_d and e_r are the void ratios of the intact, disturbed and remolded soil, respectively; $\sigma'_{v,i}$, $\sigma'_{v,d}$ and $\sigma'_{v,r}$ are the vertical effective stresses of the intact soil, disturbed soil and remolded soil, respectively; $\sigma'_{h,i}$, $\sigma'_{h,d}$ and $\sigma'_{h,r}$ are the horizontal effective stresses of the intact soil, disturbed soil and remolded soil, respectively. It could be seen that i, d and r correspond to the relatively intact (RI) state, the actual response (AR) state and the fully adjusted (FA) states proposed by Desai and Toth (1996), respectively.

Eq. (4) could quantitatively evaluate the degree of soil structure disturbance under different stress states and void ratios, and is a promising way to characterize soil structure damage. Although it requires that the void ratio (or soil density) should be obtained by field testing or laboratory observations in Eqs. (5)–(7), it could be regarded as constant for the undrained condition in soft clays and thus the calculation of Eq. (4) could be simplified.

As shown in Fig. 2, the evaluation of soil structure disturbance for a specimen includes two stages: at stage I, the soil structure disturbance caused by drilled sampling process in the field; at stage II, the further disturbance occurred during the subsequent consolidation of the disturbed sample in laboratory test. The in situ shear wave velocity could be measured by crosshole, downhole or a portable bender element-double cone penetration testing equipment before soil sampling in the field (e.g. Tong et al., 2018; Barus et al., 2019; Kang et al., 2020). In this study, crosshole method was used to measure the in situ shear wave velocity, and the lateral pressure of in situ soil could be calculated from the effective overburden stress and the static earth pressure coefficient. Soil density and water content of the sample are measured and the corresponding initial values of the intact soil are estimated according to the rebound index from the loading-unloading curve of odometer test. For disturbed soil, the unconfined shear wave velocity of the sample could be measured by portable piezoelectric bending elements (Zhou and Chen, 2005; Orazi et al., 2018), and the residual stress could be directly measured by tensiometer. For remolded samples, multi-staged isotropic consolidation triaxial tests equipped with bender elements could be used to monitor shear wave velocity under different confining pressures, and then the parameters of Eq. (2) are determined. Note that this procedure assumes that the stress state of soil in the field or in the laboratory could be measured directly or estimated by appropriate calculation method.

3. Case study of soil sampling in soft clay deposit

Soil sampling disturbance refers to the disturbance caused by field sampling process, transportation, pushing soil samples out of the sampler and cutting sample in the laboratory, etc. Sampling inevitably causes stress release and soil structure damage. Although the influence of stress release on test results could be eliminated by confining pressure or preloading (Tan et al., 2002), structure disturbance caused by sampling could not be recovered in laboratory tests. Therefore, the evaluation of sampling quality mainly focuses on soil structure disturbance. Eq. (4) was used to evaluate sampling disturbance caused by open end thin-wall sampler at a construction site in Ningbo City, Zhejiang Province, China. The in situ wave velocity test was measured before soil sampling in the field, and the unconfined wave velocity and residual stress were measured after sampling in the laboratory.

3.1. Field testing and soil sampling

The test site is located in the suburb of Ningbo City. The deep soft clay deposit is mainly composed of typical structured soft clays with high moisture content, high compressibility, low shear strength and poor permeability. The in situ wave velocity measurement and soil sampling were carried out in sequence on site. The layout of crosshole seismic testing and soil sampling is shown in Fig. 3.

Fig. 4 shows the typical signal of crosshole seismic testing, and the first arrival point could be identified by the reversible polarization of shear waves. The shear wave velocity is calculated according to the following equation:

$$V_s = L/t_s \tag{8}$$

where L is the horizontal distance between two boreholes, and t_s is the propagation time of the shear wave.

After the measurement in situ shear wave velocity, an open end thin-wall sampler similar to Shelby tube was used for soil sampling (Wang et al., 2019). The thin-wall tube has a diameter of 10 cm and a length of 75 cm. The end of the thin-wall tube is polished into a cutting edge and Vaseline is smeared on the inner wall of the tube to reduce the friction resistance during sampling. The sampling

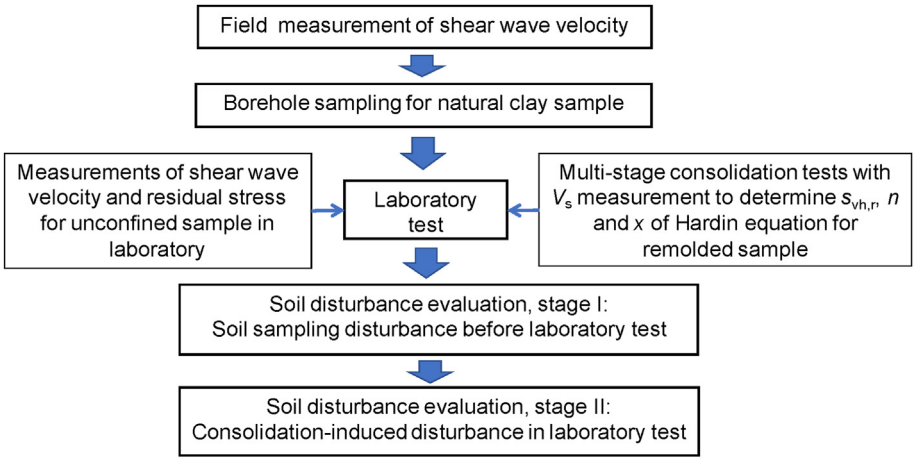

Fig. 2. Flow chart for soil disturbance evaluation based on stress-normalized stiffness.

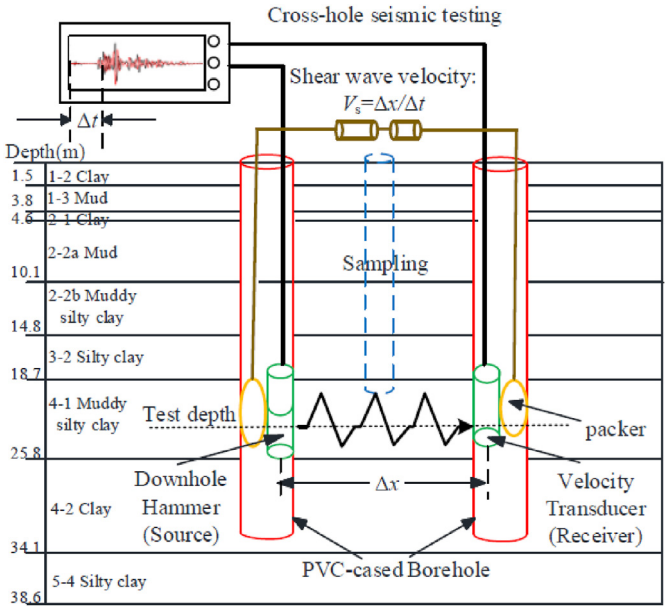

Fig. 3. Crosshole seismic testing and soil sampling arrangement in the field.

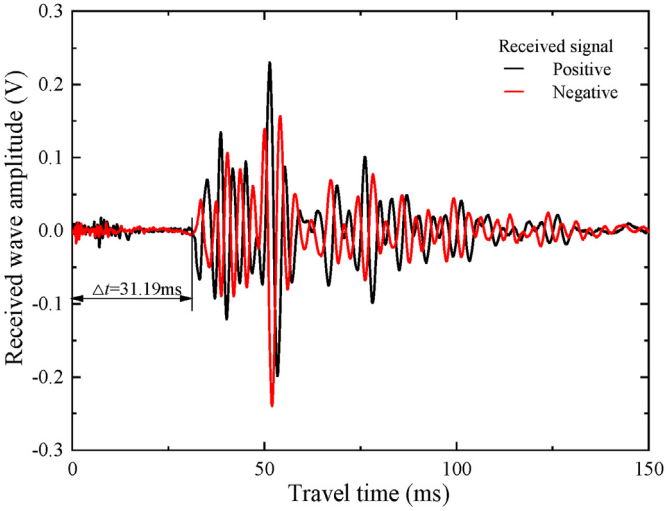

Fig. 4. Typical shear wave signals by crosshole method in the field.

depth ranged from 4 m to 25 m with an interval of 3 m. During sampling, the sampler shall be penetrated in a rapid and continuous static pressure mode. After sampling, both ends of the thin-wall tube were sealed with matching rubber caps and then wax was coated to prevent water evaporation of the soil sample. After transporting to the laboratory, the soil sample at a specific depth was pushed out from the thin-wall sampler and the physical and mechanical properties of the soil were measured. The results are given in Table 1. Sampling, storage, transportation and testing were conducted according to ASTM standard procedures (ASTM D4220/D4200M-14, 2014; ASTM D1587/D1587M-15, 2015; ASTM D4318-17e1, 2017).

3.2. Laboratory tests

Laboratory isotropic consolidation tests of remolded samples of soil layers 2–1, 2-2a, 3–2 and 4–1 were carried out on a GDS triaxial apparatus equipped with bender element system. The sample is 50 mm in diameter and 100 mm in height (Fig. 5). The procedure for preparing reconstituted specimens is briefly introduced as follows: firstly, soil samples were dried and crushed in to powder, and then compacted in five layers to the desired dry density in a cylindrical mould with inner geometries of 50 mm in diameter and 100 mm in height; then the specimen was saturated by vacuum method for 24 h; finally, the saturated specimen was moved to the pedestal of triaxial apparatus for the desired consolidation.

The multiple-staged loading sequence of isotropic consolidation is from 25 kPa to 400 kPa. After loading to 400 kPa, samples were gradually unloaded to 25 kPa (ASTM D4767, 2011). After each stage of consolidation was completed, bender elements were used to measure the shear wave velocity. Typical signals are shown in Fig. 6.

Fig. 7 shows the e-$\log_{10}p'$ and $\log_{10}G_{max}$-$\log_{10}p'$ curves of remolded samples from 2-2a layer. Under the condition of loading and unloading, the compression curve of the remolded sample is roughly straight without structural yield stress (i.e. σ'_y). The structural yield stress of natural soft clay could be defined as the stress level beyond which the compression curve has typical softening characteristics with significant plastic deformation (e.g. Huang et al., 2011). This indicates that the natural structure of the soil has been basically destroyed after drying, crushing and sample preparation. The void ratio function Eq. (3) is substituted into Eq. (2), and the logarithm of both sides leads to

$$\log_{10}G_{max} = \log_{10}\left[S_{vh}P_a^{(1-2n)}\right] + n\log_{10}(\sigma'_v\sigma'_h) - x\log_{10}e \tag{9}$$

Then the parameters of $S_{vh,r}$, n and x could be obtained by fitting $\log_{10}G_{max}$-$\log_{10}p'$, and n and x will be further used in subsequent isotropic consolidation of the disturbed soil sample. Fig. 8 shows the relationship between $\log_{10}G_{max}/F(e)$ and $\log_{10}(\sigma'_v\sigma'_h)$ for remolded samples of all sub-layers. There is a good linear correlation in the double-logarithmic space. The parameter $S_{vh,r}$ of four remolded soils varies from 300 to 360 in a narrow range, and the exponent n also stays around 0.25 (Stokoe and Santamarina, 2000).

The drilled soil sample at specific depth was pushed out from the sampler and cut into a 120 mm length specimen by a wire saw. Firstly, bender elements were used to measure the unconfined shear wave velocity. Fig. 9 shows the portable bender element testing system developed at Zhejiang University. The penetrating length of bender element into soil sample is 10 mm, the travel distance of shear wave is about 100 mm, and the excitation frequency varies from 0.4 kHz to 1 kHz. Fig. 10 shows a typical signal of portable bender elements for a soil sample at a depth of 13 m. The traveling time of shear waves is determined by "time domain first arrival method", which treats the first distinct upward deflection as the arrival of shear wave (i.e. point R in Fig. 10) and T-R span as the travel time (Yamashita et al., 2009). After the measurement of unconfined wave velocity, the corresponding residual stress of the same soil sample was measured by 2100F tensiometer produced by Soil Moisture Corporation in the United States (Donohue and Long, 2009). Figs. 11 and 12 shows the profiles of shear wave velocities and the residual stresses of the drilled samples, respectively. Due to stress release and soil structure disturbance during sampling, the unconfined shear wave velocity is much less than the field value, and the residual stress is only about 10% of the effective overburden stress.

3.3. Soil sampling disturbance evaluation

Due to the stress release during sampling, the soil sample inevitably rebounds. It changes the void ratio and it is necessary to

Table 1
Physical and mechanical properties of soil strata.

Soil strata	Depth (m)	Natural soil density (g/cm^3)	Water content (%)	Liquid limit (%)	Void ratio	Rebound index	Coefficient of earth pressure at rest	Sensitivity
2-1: Clay	3.8–4.6	1.81	43	40	1.214	0.057	0.59	3.9
2-2a: Silt	4.6–10.1	1.62	41.5	39.5	1.388	0.069	0.6	3.7
2-2b: Muddy silty clay	10.1–14.8	1.76	43.5	36	1.208	0.051	0.51	3.4
3-2: Silty clay	14.8–18.7	1.86	32.7	28	0.936	0.024	0.44	3.3
4-1: Muddy silty clay	18.7–25.8	1.8	38.7	33.2	1.079	0.043	0.52	3.4
4-2: Clay	25.8–34.1	1.74	43.5	45	1.282	0.058	0.55	3

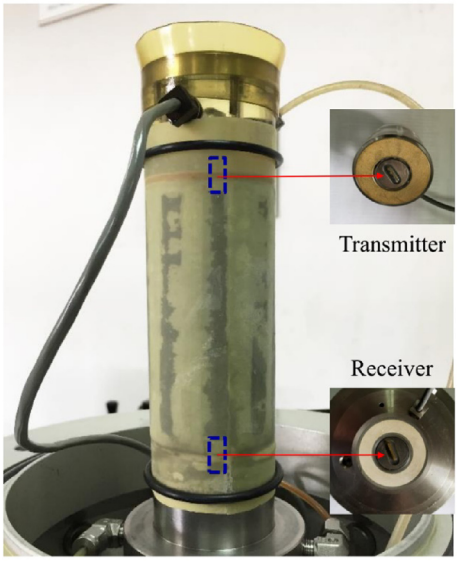

Fig. 5. Specimen in triaxial apparatus with bender elements.

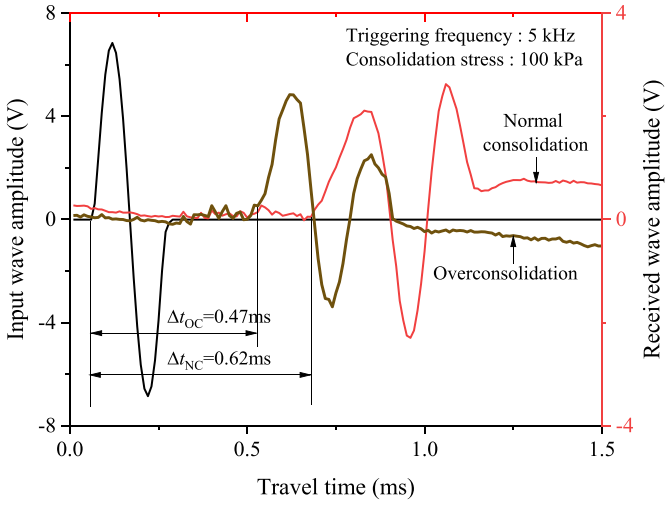

Fig. 6. Typical signals of bender element testing in triaxial apparatus.

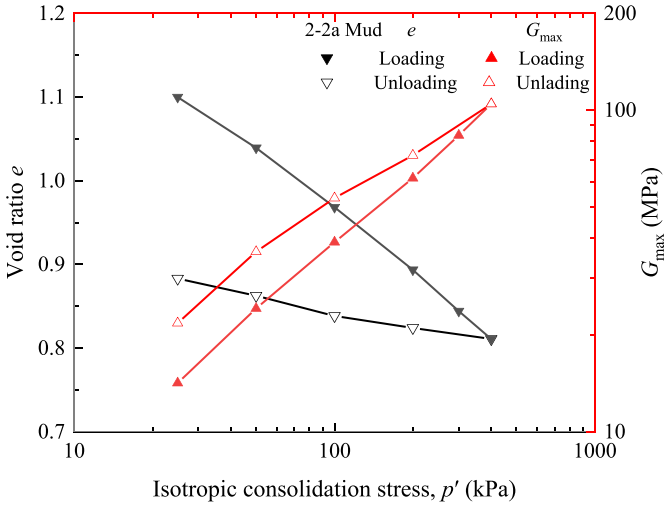

Fig. 7. Variations of e, G_{max} with p' for 2-2a remolded soil.

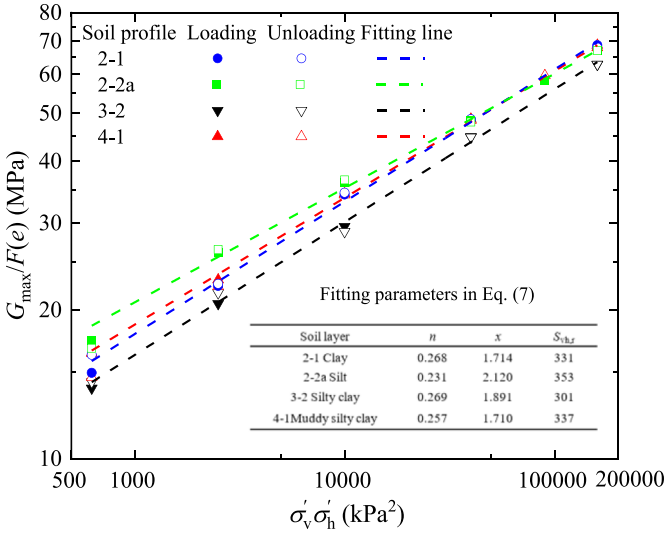

Fig. 8. Variation of $G_{max}/F(e)$ with p' for all remolded soil samples.

estimate the in situ void ratio at intact state. According to one-dimensional compression theory (Schmertmann 1955), the in situ void ratio and density are estimated as follows:

$$e_i = e_d - C_s \log_{10}\left(\frac{\sigma'_{v0}}{\sigma'_r}\right) \quad (10)$$

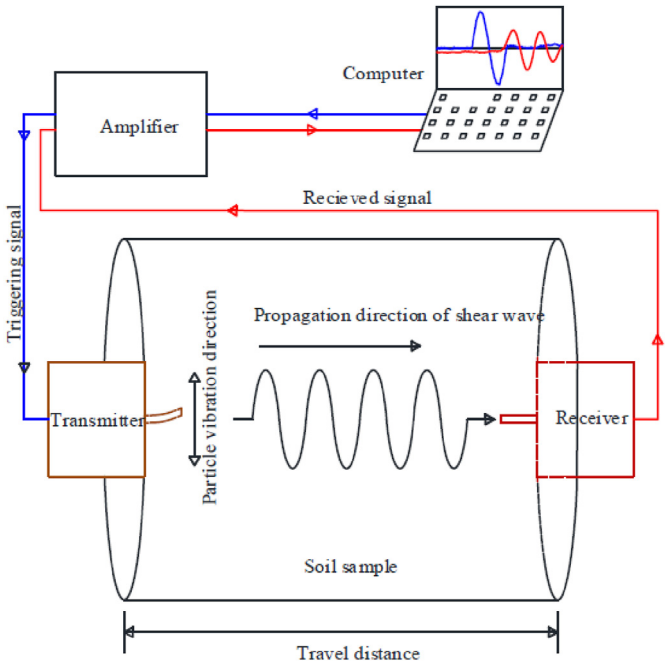

Fig. 9. Schematic diagram of portable bender element test.

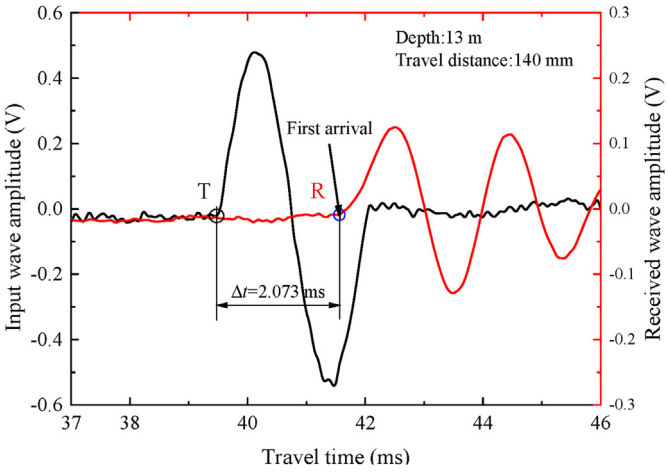

Fig. 10. Typical signals of portable bender element test.

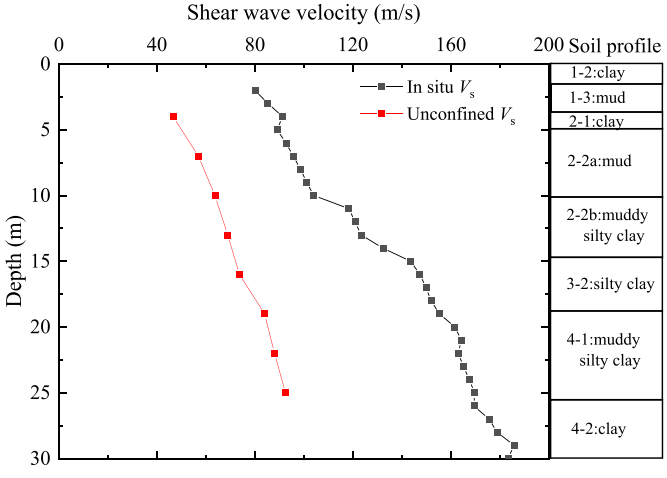

Fig. 11. V_s comparison between the unconfined sample and the in situ soil.

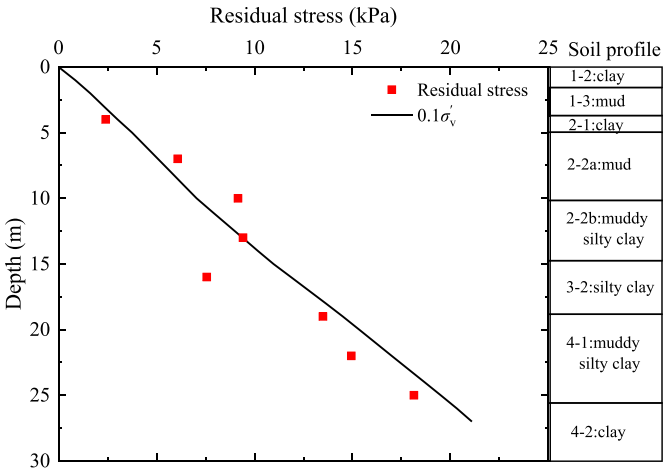

Fig. 12. Residual stress of soil samples collected by open end thin-wall sampler.

Table 2
Soil disturbance degree determined by the proposed procedure (Eq. (4)).

Soil strata	Depth (m)	Soil disturbance degree (%)
2-1 Clay	4	28.5
2-2a Silt	7	29.9
2-2a Silt	10	32.9
2-2b Muddy silty clay	13	31.3
3-2 Silty clay	16	28.6
4-1 Muddy silty clay	19	33.2
4-1 Muddy silty clay	22	27.3
4-1 Muddy silty clay	25	30

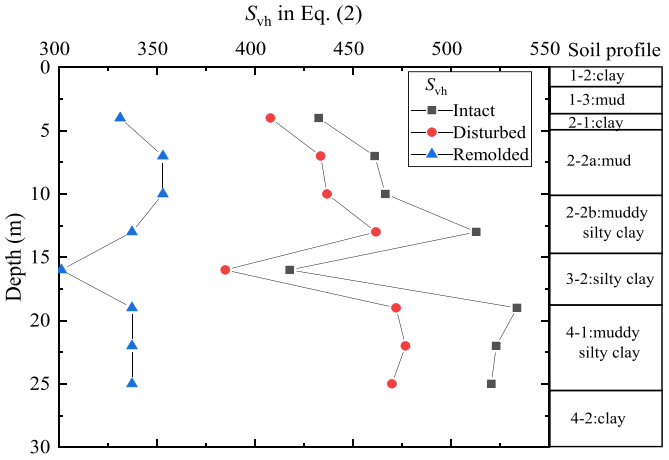

Fig. 13. Soil structure parameter S_{vh} at different soil layers in the field.

where e_i is the in situ void ratio, e_d is the void ratio after sampling, C_s is the recompression index, σ'_{v0} is the effective overburden stress, σ'_r is the residual stress, and ρ_i is the in situ soil density at intact state:

$$\rho_i = \frac{\rho_d(1+e_d)}{1+e_i} \tag{11}$$

where ρ_d is the soil density after sampling at disturbed state.

The structure parameter of the intact in situ soil and the disturbed soil are calculated according to Eqs. (5) and (6), respectively, and the results are shown in Fig. 13. The degree of soil structure disturbance is calculated according to Eq. (4), and the

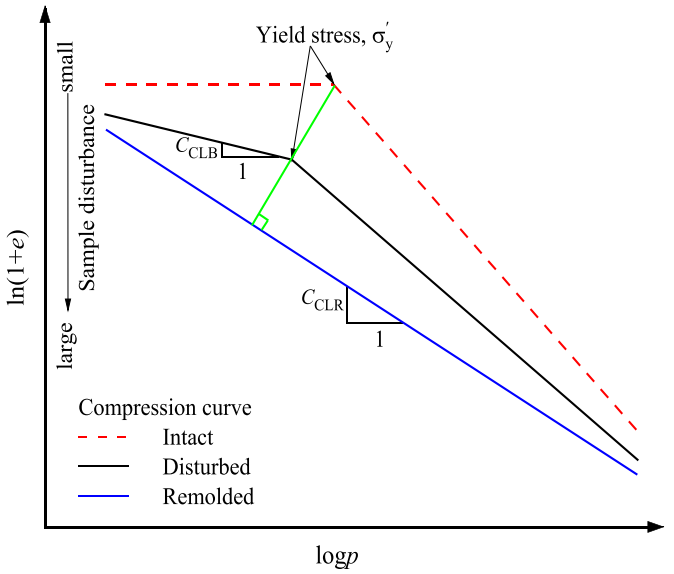

Fig. 14. Schematic diagram of sample disturbance based on compression curve (modified from Hong and Onitsuka, 1998).

results are given in Table 2. The degree of soil structure disturbance at different depths is about 30%, which implies that the structure disturbance is mainly affected by sampling method and not considerably affected by sampling depth or soil sub-layer.

In order to verify the rationality of the present procedure to evaluate soil sampling disturbance, the modified volume compression method proposed by Hong and Onitsuka (1998) was used as a reference. On the basis of the inherent compression line of remolded soil proposed by Burland (1990), Hong and Onitsuka (1998) proposed a method to evaluate sample disturbance as follows:

$$SD_{\mathrm{d}} = \frac{C_{\mathrm{CLB}}}{C_{\mathrm{CLR}}} \times 100\% \tag{12}$$

where C_{CLB} is the compression index of disturbed soils before yielding in the ln $(1 + e)$-$\log_{10}p$ plot, and C_{CLR} is the compression index of remolded soils in the ln $(1 + e)$-$\log_{10}p$ plot.

Fig. 14 conceptually shows the effect of sample disturbance on compression curves, where SD_{d} directly corresponds to the plastic volumetric strain and reflects the degree of soil structure damage. SD_{d} will vary from 0 (intact) to 100% (completely remolded). Fig. 15 shows the ln $(1 + e)$-$\log_{10}p$ curve obtained from the standard consolidation test of soil samples at different depths. C_{CLB} and C_{CLR} are obtained by fitting compression curves of the disturbed and the remolded samples respectively. The sampling disturbance degree is calculated according to Eq. (12) and given in Table 3, which varies from 20% to 30%.

Fig. 16 shows the comparison between the two methods. The results of two methods are close to each other, despite that the result of normalized shear modulus is slightly higher than that of the modified volume method. It is possibly related to the determination of rebound index (Boone, 2010; Butterfield, 2011), which may lead to a higher estimation of soil disturbance by the proposed procedure.

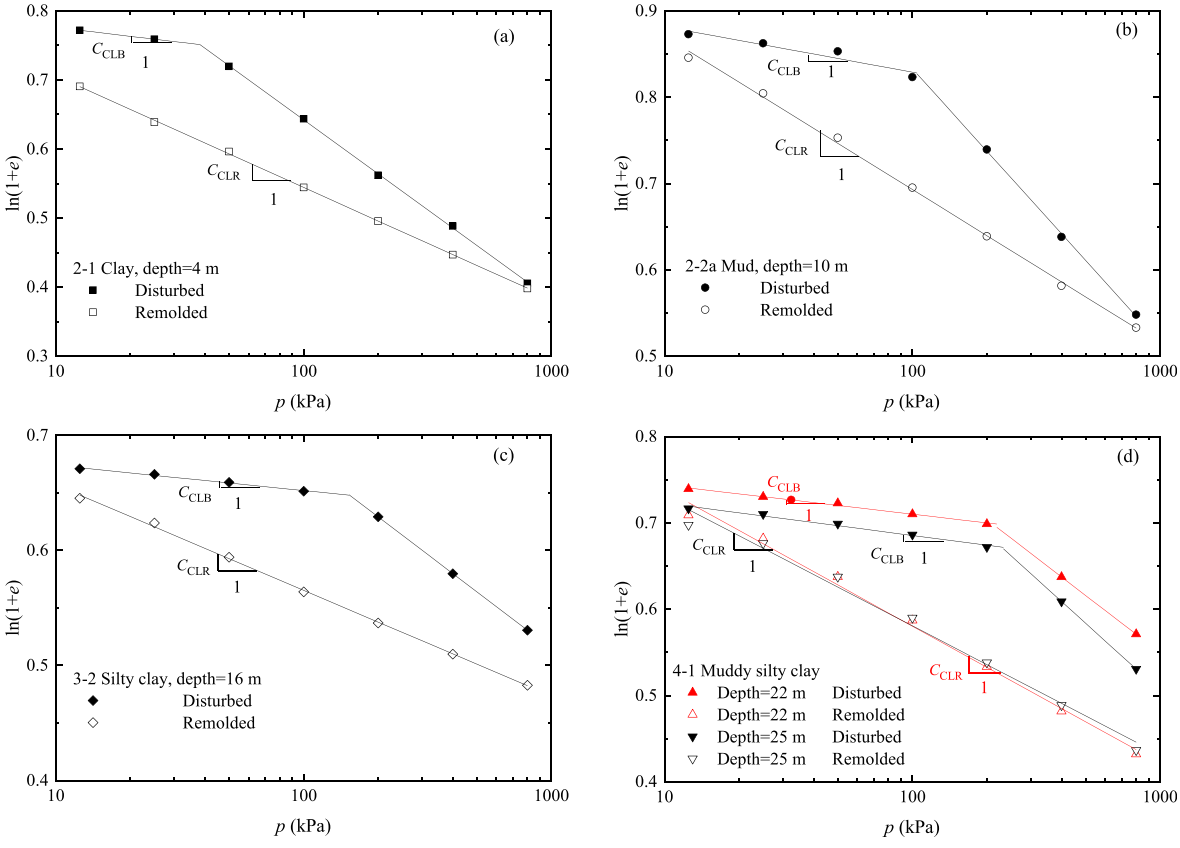

Fig. 15. Compression curves of natural and remolded soil samples.

Table 3
Sample disturbance degree from Hong and Onitsuka (1998) method.

Depth (m)	Structural yield stress (kPa)	C_{CLB} (10^{-2})	C_{CLR} (10^{-2})	*SDD* (%)
4	38.15	4.29	16.16	26.5
10	104.4	5.26	17.79	29.6
16	152.5	2.19	9.17	23.9
22	219.2	3.36	15.85	21.2
25	233.1	3.75	14.92	25.1

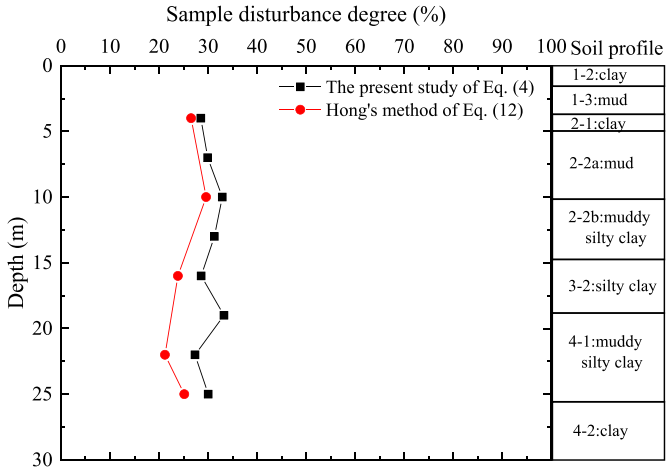

Fig. 16. Comparison of soil disturbance degree obtained from two methods.

3.4. Evaluation of further disturbance during consolidation

The isotropic consolidation test of the disturbed natural sample of 2-2a layer was carried out on a GDS triaxial apparatus equipped with bender elements. The initial void ratio of the disturbed sample was the same as that of the remolded one. The multi-staged loading sequence is the same as that for the remolded sample, which is from 25 kPa to 400 kPa. Fig. 17 shows the e-$\log_{10}p'$ and $\log_{10}G_{max}$-$\log_{10}p'$ curve for 2-2a layer. Compared with the remolded sample, the compression curve of the disturbed natural sample shows obvious structural feature and has a structural yield stress. With the increase of consolidation pressure, the compression of disturbed natural sample increases significantly and its compression curve gradually approaches to that of the remolded one. Then the in situ vertical effective stress and the structural yield stress were obtained respectively according to the method proposed by Wang and Li (2007).

According to Fig. 8, the void ratio function $F(e) = e^{-2.12}$ is used to normalize the small-strain shear modulus of the disturbed natural sample at 2-2a layer. Fig. 18 shows the relationship between $\log_{10}G_{max}/F(e)$ and $\log_{10}(\sigma'_v\sigma'_h)$ for this layer. When the consolidation pressure exceeds the effective overburden stress, the $G_{max}/F(e)$ of the disturbed sample gradually approaches to that of the remolded one.

With the data in Fig. 18, Eq. (2) is used to calculate the structure parameters of the disturbed sample under different consolidation stresses. Fig. 19 shows the relationship between the structure parameters ($S_{vh,d}$) and the consolidation pressure (p'). When the consolidation pressure (p') is less than the in situ vertical effective stress (σ'_{v0}), the disturbed sample is still at the state of recompression, and the structure parameters ($S_{vh,d}$) changes slightly. According to Eq. (4), the soil disturbance degree before applying consolidation pressure is $SDD = 36.3\%$, which stands for the accumulated disturbance from the soil sampling and the installation into the triaxial apparatus. When the consolidation pressure (p') is

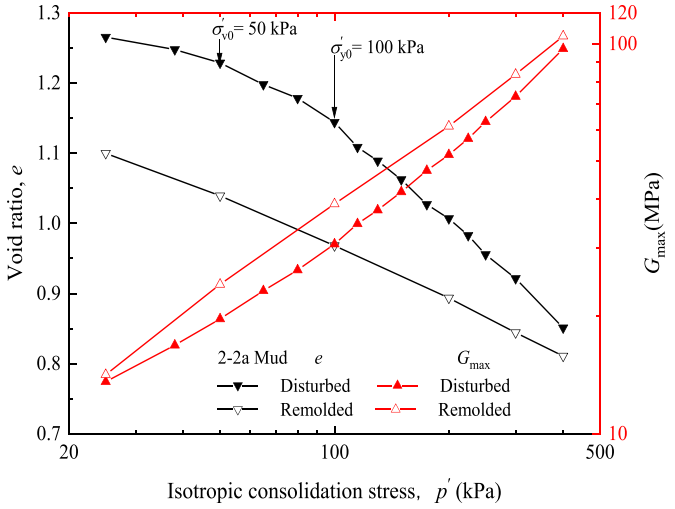

Fig. 17. Comparison between the natural and remolded samples of layer 2-2a.

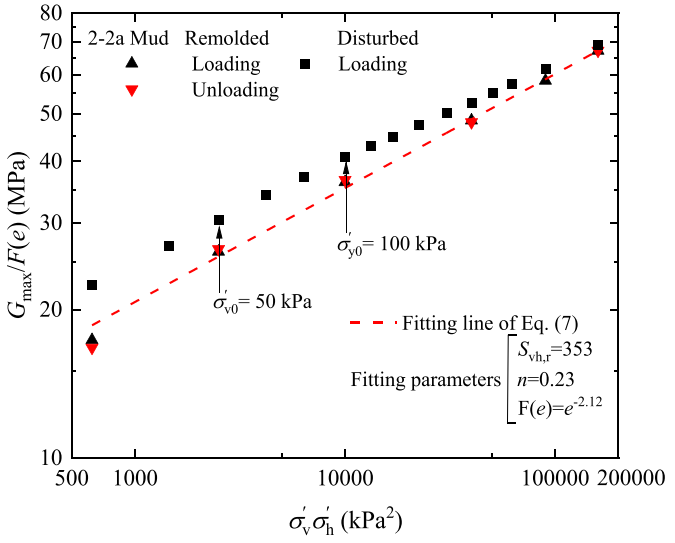

Fig. 18. Relationship between G_{max} and confining pressure.

between the in situ vertical effective stress (σ'_{v0}) and the structural yield stress (σ'_v), the structure parameter ($S_{vh,d}$) begins to decrease considerably. The soil structure is damaged to some extent, but the structure parameter ($S_{vh,d}$) is still far greater than the corresponding value of remolded soil ($S_{vh,r}$). When the consolidation pressure (p') is far beyond the structural yield stress (σ'_y), the structure parameter ($S_{vh,d}$) decreases continuously, and then stabilizes near a value slightly larger than the corresponding remolded soil ($S_{vh,r}$). In this stage, soil structure is heavily damaged. Large plastic volumetric strain occurs and the metastable structure of disturbed soil has been basically deconstructed.

With the data in Fig. 19, the degree of soil structure disturbance is calculated by Eq. (4), and two curves are drawn according to whether the initial soil sampling disturbance is included or not. The plastic volume strain (ε_p) is calculated according to the void ratio at each loading stage. The results are shown in Fig. 20. The soil disturbance degree (*SDD*) calculated by Eq. (4) is consistent with the structure damage characterized by plastic volume strain (ε_p). In the stage of recompression, ε_p is small, and corresponding *SDD* is also small. When the consolidation pressure (p') exceeds the in situ

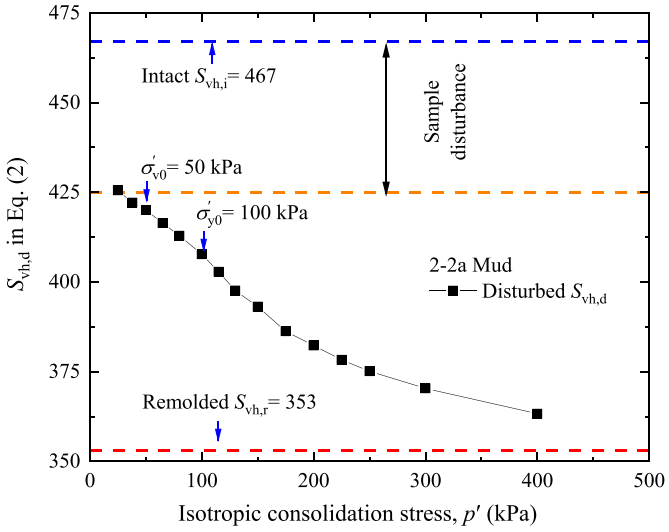

Fig. 19. Continuous decrease of S_{vh} during multi-staged consolidation.

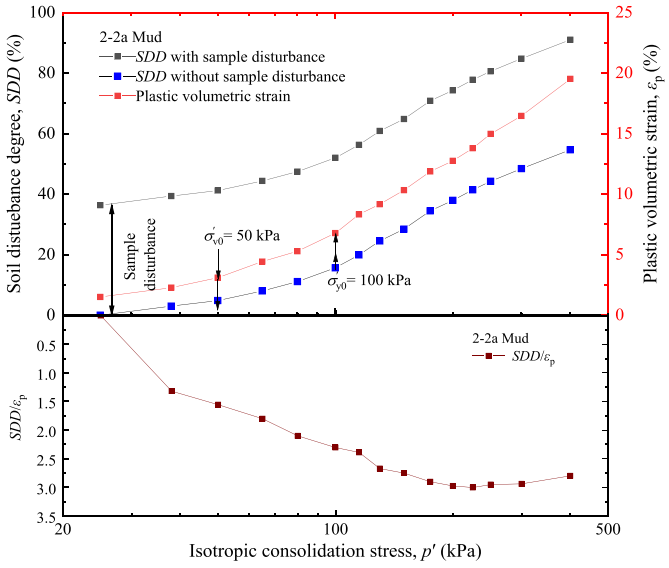

Fig. 20. Variations of SDD and volumetric strain during multi-staged consolidation.

vertical effective stress (σ'_{v0}), the development of ε_p begins to accelerate. The metastable structure of the sample begins to deconstruct, so *SDD* starts to increase. When the consolidation pressure (p') is greater than the structural yield stress (σ'_y), the plastic volume strain develops rapidly and the soil structure damage is aggravated. It is interesting to find that the soil disturbance degree follows the plastic volumetric strain quite well during consolidation, and the ratio between SDD and volumetric strain is about 1.5 when the consolidation stress is less than the structural yield stress while it approaches 3.0 when the consolidation stress is higher than the structural yield stress for the studied soil layer.

4. Conclusions

In the present study, the small-strain shear modulus is used to characterize soil structure disturbance by normalizing the effective stress and void ratio based on Hardin equation. The procedure for evaluating soil sampling disturbance in the field and the further disturbance during the subsequent consolidation process in laboratory test is proposed, and then validated by an engineering case study of typical soft clay ground. Some major findings are given below:

(1) The small-strain shear stiffness, or shear wave velocity, could represent the initial structure state of soil at any disturbed state. Therefore, it is a constant-fabric measurement at a given state of stress. The shear wave velocity could be reliably monitored from the field to the laboratory by crosshole seismic testing at the ground, portable piezoelectric bender elements for the drilled sample and bender elements equipped in triaxial apparatus for the sample under consolidation in the present study.

(2) It is found that soil sampling disturbance degree by the open end thin-wall sampler is about 20%–30% according to the proposed procedure, which is slightly higher than the modified volume compression method proposed by Hong and Onitsuka (1998). As the Hong and Onitsuka method is defined based on plastic volumetric strain and could be regarded as the physically proper reference method, the comparison proves the applicability of the proposed stress-normalized small-strain shear stiffness to evaluate the sampling disturbance.

(3) The applicability of this procedure for evaluating additional soil disturbance during the subsequent consolidation process in laboratory test was further studied by consolidation tests in triaxial apparatus equipped with bender elements. When the consolidation pressure exceeds the structural yield stress, the metastable structure of the disturbed sample is further damaged gradually and it could be evaluated by the parameter S_{vh}. The additional soil disturbance degree under consolidation pressure of 400 kPa could reach about 50% according to the present study, and it follows the plastic volumetric strain quite well during multi-staged consolidation.

Declaration of competing interest

The authors declare that they have no known competing financial interests or personal relationships that could have appeared to influence the work reported in this paper.

Acknowledgments

This study is partly supported by the National Natural Science Foundation of China (Grant Nos. 51978613, 52278374 and 51988101). All these funding grants are greatly acknowledged.

References

ASTM D1587/D1587M-15, 2015. Standard Practice for Thin-Walled Tube Sampling of Fine-Grained Soils for Geotechnical Purposes. ASTM International, West Conshohocken, PA, USA.
ASTM D4220/D4200M-14, 2014. Standard Practices for Preserving and Transporting Soil Samples. ASTM International, West Conshohocken, PA, USA.
ASTM D4318-17e1, 2017. Standard Test Methods for Liquid Limit, Plastic Limit, and Plasticity Index of Soils. ASTM International, West Conshohocken, PA, USA.
ASTM D4767, 2011. Standard Test Method for One-Dimensional Consolidation Properties of Soils Using Incremental Loading. ASTM International, West Conshohocken, PA, USA.
Barus, R.M.N., Jotisankasa, A., Chaiprakaikeow, S., Sawangsuriya, A., 2019. Laboratory and field evaluation of modulus-suction-moisture relationship for a silty sand subgrade. Transp. Geotech. 19 (2), 126–134.
Boone, S.J., 2010. A critical reappraisal of "preconsolidation pressure" interpretations using the oedometer test. Can. Geotech. J. 47 (3), 281–296.
Burland, J.B., 1990. On the compressibility and shear strength of natural clays. Geotechnique 40 (3), 329–378.

Butterfield, R., 2011. An improved model of soil response to load, unload and re-load cycles in an oedometer. Soils Found. 51 (2), 253–263.
Dadashiserej, A., Jana, A., Ortiz, S.C., Walters, J.J., Stuedlein, A.W., Evans, T.M., 2022. Monotonic, cyclic, and post-cyclic response of Willamette River silt at the van buren Bridge. In: Proceedings of the Geo-Congress 2022: Geophysical and Earthquake Engineering and Soil Dynamics. Geotechnical Special Publication No. 334, ASCE, Reston. VA, pp. 431–443.
DeJong, J.T., Krage, C.P., Albin, B.M., DeGroot, D.J., 2018. Work-based framework for sample quality evaluation of low plasticity soils. J. Geotech. Geoenviron. Eng. 144 (10), 04018074.
Desai, C., Toth, J., 1996. Disturbed state constitutive modeling based on stress-strain and nondestructive behavior. Int. J. Solid Struct. 33 (11), 1619–1650.
Donohue, S., Long, M., 2009. Suction measurements as indicators of sample quality in soft clay. Geotech. Test J. 32 (3), 286–296.
Hardin, B.O., Blandford, G.E., 1989. Elasticity of particulate materials. J. Geotech. Eng. 115 (6), 788–805.
Hight, D.W., Leroueil, S., 2002. Characterization of soils for engineering purposes. Characterisation and Engineering Properies of Natural Soils 1, 255–360. Singapore.
Hong, Z.S., Onitsuka, K., 1998. A method of correcting yield stress and compression index of Ariake clays for sample disturbance. Soils Found. 38 (2), 211–222.
Hong, Z.S., Zeng, L., Cui, Y., Lin, Y., 2012. Compression behaviour of natural and reconstituted clays. Geotechnique 62 (4), 291–301.
Huang, M., Liu, Y., Sheng, D., 2011. Simulation of yielding and stress–stain behavior of shanghai soft clay. Comput. Geotech. 38 (3), 341–353.
Jamiolkowski, M., Lancellotta, R., Presti, D.C.F.L., 1995. Remarks on the stiffness at small strains of six Italian clays. Dev. Deep Found. Gr. Improv. Schemes 197–216.
Jana, A., Stuedlein, A.W., 2020. Monotonic, cyclic, and postcyclic responses of an alluvial plastic silt deposit. J. Geotech. Geoenviron. Eng. 147 (3), 4020174-4020118.
Kang, X., Sun, H.M., Luo, H., Dai, T., Chen, R.P., 2020. A portable bender element-double cone penetration testing equipment for measuring stiffness and shear strength of in situ soft soil deposits. KSCE J. Civ. Eng. 24 (12), 3546–3560.
Khalid, U., Ye, G., Yadav, S., Zhou, A., Gu, L., 2021. Consolidation pressure consequences on the soil structure of artificial structured marine clay: macro and micro evaluation. Geotech. Geol. Eng. 39 (1), 1–17.
Landon, M.M., DeGroot, D.J., Sheahan, T.C., 2007. Nondestructive sample quality assessment of a soft clay using shear wave velocity. J. Geotech. Geoenviron. Eng. 133 (4), 424–432.
Li, Y., Otsubo, M., Kuwano, R., 2023. Evaluation of soil fabric using elastic waves during load-unload. J. Rock Mech. Geotech. Eng. 15 (10), 2687–2700.
Lo Presti, D.C.F.L., 1989. Proprietà Dinamiche dei Terreni. In: Proceedings of the XIV Conference on Geotechnology, pp. 1–62 di Torino.
Low, H.E., Phoon, K.K., 2008. Effect of cementation on the compressibility of Singapore upper marine clay. Can. Geotech. J. 45 (7), 1018–1024.
Lunne, T., Berre, T., Andersen, K.H., Strandvik, S., Sjursen, M., 2006. Effects of sample disturbance and consolidation procedures on measured shear strength of soft marine Norwegian clays. Can. Geotech. J. 43 (7), 726–750.
Mitchell, R.J., 1970. On the yielding and mechanical strength of Leda clays. Can. Geotech. J. 7 (3), 297–312.
Nagaraj, T.S., Miura, N., Chung, S.G., Prasad, K.N., 2003. Analysis and assessment of sampling disturbance of soft sensitive clays. Geotechnique 53 (7), 679–683.
Orazi, M., Gori, U., Ruggeri, P., Sakellariadi, E., Scarpelli, G., 2018. Small-strain stiffness values for a reconstituted soil from southern Italy. Geotech. Geol. Eng. 36 (4), 1–8.
Rampello, S., Callisto, L., 1998. A study on the subsoil of the Tower of Pisa based on results from standard and high-quality samples. Can. Geotech. J. 35 (6), 1074–1092.
Santamarina, J.C., Klein, A., Fam, M.A., 2001. Soils and waves: particulate materials behavior, characterization and process monitoring. J. Soils Sediments 1 (2), 130, 130.
Schmertmann, J.H., 1955. The undisturbed consolidation behavior of clay. Trans. ASCE. 120, 1201–1233.
Shibuya, S., 2000. Assessing structure of aged natural sedimentary clays. Soils Found. 40 (3), 1–16.
Shibuya, S., Hwang, S.C., Mitachi, T., 1997. Elastic shear modulus of soft clays from shear wave velocity measurement. Geotechnique 47 (3), 593–601.
Stokoe, K.H., Santamarina, J.C., 2000. Seismic-wave-based testing in geotechnical engineering. In: International Conference on Geotechnical and Geological Engineering. GeoEng 2000, Melbourne, Australia, pp. 1490–1536.
Tan, T.S., Lee, F.H., Chong, P.T., Tanaka, H., 2002. Effect of sampling disturbance on properties of Singapore clay. J. Geotech. Geoenviron. Eng. 128 (11), 898–906.
Tanoli, A., Ye, G., 2021. Numerical modeling of excavation in Shanghai soft clays using the new small strain Shanghai constitutive Model. In: GeoChina 2021, pp. 80–94.
Tong, L.Y., Che, H.B., Zhang, M.F., Pan, H.S., 2018. Determination of shear wave velocity of Yangtze Delta sediments using seismic piezocone tests. Transp. Geotech. 14, 29–40.
Viggiani, G., Atkinson, J.H., 1995. Stiffness of fine-grained soil at very small strains. Geotechnique 45 (2), 249–265.
Wang, L.Z., Li, L.L., 2007. Field disturbance of structured clay and its effect on settlements of soil foundation. Chin. J. Geotech. Eng. 29 (5), 697–704 (in Chinese).
Wang, J., Feng, D., Guo, L., Fu, H., Cai, Y., Wu, T., Shi, L., 2019. Anisotropic and noncoaxial behavior of K0-consolidated soft clays under stress paths with principal stress rotation. J. Geotech. Geoenviron. Eng. 145 (9), 04019036.
Xiong, Y., Yang, Q., Zhang, S., et al., 2018. Thermo-elastoplastic model for soft rock considering effects of structure and overconsolidation. Rock Mech. Rock Eng. 51 (3), 3771–3784.
Yamashita, S., Kawaguchi, T., Nakata, Y., Mikami, T., Fujiwara, T., Shibuya, S., 2009. Interpretation of international parallel test on the measurement of Gmax using bender elements. Soils Found. 49 (4), 631–650.
Zeng, L.L., Hong, Z.S., 2015. Experimental study of primary consolidation time for structured and destructured clays. Appl. Clay Sci. 116–117C, 141–149.
Zhou, Y.G., Chen, Y.M., 2005. Influence of seismic cyclic loading history on small strain shear modulus of saturated sands. Soil Dynam. Earthq. Eng. 25 (5), 341–353.

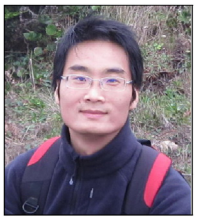

Yanguo Zhou is currently full professor in College of Civil Engineering and Architecture, Zhejiang University, China. Prof. Zhou obtained his BSc degree in Civil Engineering in 2001 and his PhD in Geotechnical Engineering in 2007, both from Zhejiang University, China. Then he became a faculty member of Department of Civil Engineering, Zhejiang University, since 2007. He worked as visiting associate researcher in Department of Civil and Environmental Engineering, University of California, Davis, from 2011 to 2014. He is now the council member of Seismological Society of China, the committee member of the International Society for Soil Mechanics and Geotechnical Engineering TC104 (Physical Modeling) and TC304 (Reliability). His research interests include (1) soil dynamics and geotechnical earthquake engineering with emphasis on soil liquefaction and mitigation; (2) soil testing and foundation engineering with emphasis on soil disturbance; and (3) hypergravity experiment by centrifuge shaking table test. He has been participated in a number of national research projects and consulted several major engineering projects.